Water Practice & Technology

IWA PUBLISHING



Water Practice & Technology Vol 17 No 10, 2083 doi: 10.2166/wpt.2022.108

# Numerical effect of seismic force on a medium arch dam

Milad Khatib [a,*], Melissa Loutfi[a], Hani Hamdan[b] and Wahib Arairo [c]

[a] Department of Civil Engineering, ISSEA-Cnam, Zkak Blat Maurice Barres, Beirut, Lebanon
[b] Université Paris-Saclay, CentraleSupélec, CNRS, Laboratoire des Signaux et Systèmes, L2S UMR CNRS 8506, Gif-sur-Yvette, France
[c] Civil Engineering and Construction Technology Department, University of Balamand, Kalhat, Al-Kurah, Lebanon
*Corresponding author. E-mail: milad.khatib@isae.edu.lb

MK, 0000-0002-0140-0941; WA, 0000-0002-1708-0233

## ABSTRACT

The dam is considered a huge structure that has multiple purposes in the life of a human. The most important role of a dam is the production of electricity, and the storage of a huge quantity of water. Therefore, it is very important to be vigilant in the studies made for it. Lebanon has indeed been designated as a seismicity country. However, the number of dams is increasing due to several natural consideration. Mseilha dam is an executed medium arch dam, which faced several problems during and after construction. The initial problem that faced a dam is the seismic force. This natural force is very dangerous for any structure, especially for a dam. It could increase the existing concrete stresses. These stresses will cause the development of cracks all along the dam. Once the concrete shows cracks, its resistance will decrease, and it will become more vulnerable to external effects. Several studies were made to fortify it and make it resistant to seismic force. To show the major effect of this force, two methods 'pseudo-static' and 'response spectrum' were applied to a medium arch dam. Therefore, to evaluate the performance of these two methods, the dam is modelled using finite element software. The obtained results show the importance of using the appropriate model in the design of such dams without taking the appropriate model.

**Key words:** finite element software, medium arch dam, pseudo-static, response spectrum, seismic loading

## HIGHLIGHTS

- Highlight on one of the major problems that affect the stability of medium dam.
- Clarify how to analyze this catastrophic problem and prevent the losses (Humans life and economic way).
- Illustrate, through a comparison between two analysis methods, how to simulate numerically such severe problem.
- Encourage the researches to take into consideration all the existed forces during analysis and design for all dam types.

## GRAPHICAL ABSTRACT

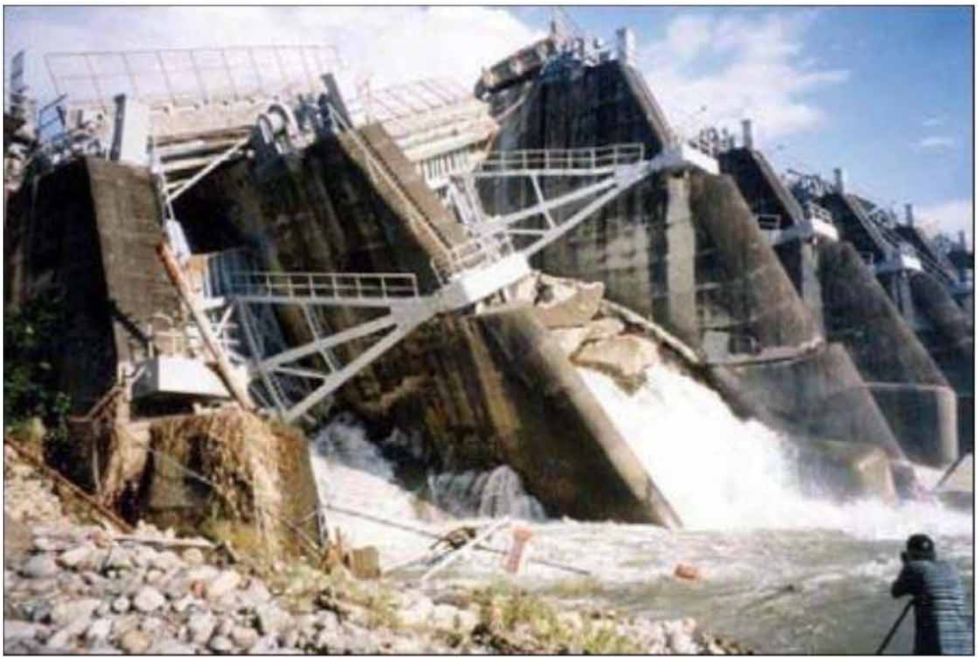

## NOMENCLATURE

| | |
|---|---|
| $E$ | Young's modulus. |
| $F$ | Hydrodynamic force. |
| $F_1$ | Seismic horizontal force. |
| $F_2$ | Seismic vertical force. |
| $G$ | Rigidity modulus. |
| $G_1$ | Sediment force. |
| $H$ | Static height of the dam. |
| $K$ | Stiffness matrix. |

| | |
|---|---|
| $L_{ca}$ | Length at the crown. |
| $L_{cb}$ | Length at the base. |
| $L_1$, $L_2$ | Lengths found in the strings of the dam. |
| M | Mass matrix. |
| P | Water pressure. |
| $P_{av}$ | Average water pressure. |
| $P_{(y)}$ | Hydrodynamic force. |
| $Q_1$ | Downstream pressure. |
| SX, SY, SZ | Stresses at each of the horizontal and vertical components of the earthquake. |
| S | Resultant of the combination of the stresses. |
| $S_T$ | Topographic coefficient. |
| $U$ | Displacement. |
| $\ddot{U}$ | Acceleration. |
| V | Volume of the concrete. |
| $a_g$ | Maximum acceleration. |
| $e_b$ | Thickness at the base. |
| $e_c$ | Thickness at crown. |
| $e_{av}$ | Average thickness. |
| h | Depth of the hold. |
| k | Pseudo-static coefficient. |
| $r_{av}$ | Average radius. |
| y | Considered depth. |
| $\alpha$ | Seismic coefficient. |
| $\sigma$ | Tensile stresses. |
| $\nu$ | Poisson's ratio. |
| $r_c$ | Radius of the dam. |
| $\gamma_b$ | Specific weight of concrete. |
| $\gamma_c$ | Compressive strength. |
| $\gamma$i | Importance coefficient. |
| $\eta$ | Depreciation correction. |
| σ | Compressive and the tensile stress. |

## 1. INTRODUCTION

An arch dam is a concrete dam that has a curved shape. The curvature shape of an arch dam allows the load of the thrust of the water to be returned to the banks. To support the rigidity of the concrete in an arch dam, the foundation should be rocky. It is necessary to evaluate the seismic force and the safety of the dam during an earthquake. An earthquake is the most dangerous force that could hit a hydraulic structure, and it is one of the most crucial concerns for engineers. A cursory examination of tectonic events in Lebanon and the Eastern Mediterranean reveals that this region of the planet has been shocked since 2000 BC by powerful earthquakes that damaged thousands of constructions and caused significant casualties and loss of life in modern-day Lebanon, Syria, Jordan, and Palestine. Lebanon has been identified as a seismically active nation. Due to the relevance of seismically active in the Eastern Mediterranean and the possible risk linked with it, various studies and research endeavors have sought to assess adjacent nations' seismic hazards (Harajli *et al.* 2002). The National Water Service Strategy, in 2010, suggested 26 dams in all. Despite the fact that the 2020 strategy attempts to reduce this number, nine dams are now under construction, and 14 more are planned for the years up to 2035 (MOE 2020). The seismic force can strongly affect the resistance of the dam, and it can be one of the important reasons for the dam's failure. For that matter, engineers and specialists considered the response of an arch dam, in the nonlinear phase, to find its critical parts that could affect the whole dam. Some easy solutions were found. According to Anton *et al.* (2019), the solution most often consists in correct the geometry of the arches, and the consoles, which implies a new iteration of the geometric definition process. Another solution was to make the arch dam more resistant to the seismic force that increases the stress, and the cracks. This solution suggests installing harnesses or crutches in the upstream part. This research shows numerically the severity of the damage that could be produced due to an earthquake, and the behaviour of a medium arch dam subjected to such force.

### 1.1. Research history and related works

The dam is considered a necessary structure in human life. Earthquakes may lead to serious damage or collapse of dams, whereas dams with huge basins can generate earthquakes. The water pressure briefly increases because of horizontal acceleration pressing towards the reservoir. The water resists movement due to its inertia as both of foundation and dam accelerate in the same direction. Aftershocks caused by earthquakes can destroy dams. Several noteworthy examples are exposed to problems and breakdowns after earthquakes.

The first example was the Lower San Fernando Dam in the USA. On 9 February 1971, this dam collapsed, due to the occurrence of liquefaction phenomena after hit by an earthquake (Lee *et al.* 1975). Numerous dams and reservoirs, in China, have been subjected to ground shaking. On 12 May 2008 due to the Wenchuan earthquake (Wieland & Houqun 2009), many dams and hydroelectric units were damaged. In 2001, an earthquake hit Bhuj city, India (Madabhushi & Haigh 2005). It caused the renovation and the fortification of 245 impacted dams. On 11 March 2011, an earthquake struck Tohoku in Japan, and 400 dams were damaged (Rajendran *et al.* 2011); also, an 18 m high embankment dam fell while eight people lost their lives.

Tan & Chopra (1995) introduced an accessible foundation approach, and computer software for the earthquake response evaluation of arch dams. This study addressed the impacts of the dam–water interface, the dam barrier absorption, and the foundation bedrock elasticity. The analysis of dam–foundation rock was developed to incorporate the contact effects with inertia, and damping. Numerical effective methods were produced to assess the most difficult element of the operation (the foundation resistance).

Hariri-Ardebili & Mirzabozorg (2013) explained the numerically the performed process for static and thermal calibration furthermore the nonlinear response of the DEZ arch dam in Khuzestan, Iran. It was explored under maximum realistic earthquake, considered joint response, break mass concrete, and possibly strengthen safety. Results reveal that the distribution of stresses will be essential inside the dam for the raised situations during earthquake forces at the maximum credible level. Based on the results, it is determined that the worst case of an arch dam being hit by an earthquake would be the case of an empty.

Chopra & ASCE M. (2012) indicated that numerous factors influence the three-dimensional study of arch dams. Those elements are the semi-unbounded size of reservoir and foundation–rock domains, dam–water interactions, wave absorption at the reservoir boundaries, water compressibility, dam–foundation rock interaction, and spatial variations in ground movement at the dam–rock interface. However, finite element calculations of arch dams undertaken in professional practice generally neglect these variables. Four-constructed arch dams in the USA (Deadwood Dam in Idaho, Monticello Dam in California, Morrow Point Dam in Colorado, and Hoover Dam in Nevada) were investigated to study the relevance of the ignored variables cited. The acquired data assured that the calculations without these parameters led to unacceptably erroneous predictions of earthquake-induced stresses. Analyses neglect spatial changes in ground movement and fail to recognize the areas of the dam that are expected to be stressed, and harmed.

Liu & Chen (2013) discussed numerically two models of the earthquake, the massless foundation and the viscous-spring conditions. The viscous-spring boundary subroutine is implemented in the finite element software ANSYS. The viscous-spring boundary and the wave input model were modelled for the seismic analysis of the Longtan gravity dam-foundation system. The obtained results demonstrate that the magnitude of the dam's dynamic reactions was less than the massless foundation model by 4%–38%. The structural dynamic reactions are overstated to some degree using the standard massless model. The radiation damping influence of infinite foundation has a major influence on the structure's dynamic responses and is highly vital to be taken into consideration.

Pan *et al.* (2015) provided an approximate incremental dynamic analysis (IDA) for the earthquake-resistant design of the Dagangshan arch dam, in China. The nonlinear seismic analysis incorporates the impacts of expansion joint opening, cracked concrete, and damped foundation. Three damage measurements related to the IDA curves were developed to assess the overall performance of arch dams. The dam endured significant damage at the dam–foundation level, and at the top level. The failure preventive performance is obtained when the transverse cracks at the top section reach the dam blocks and formed partial free cantilevers that govern the dynamic structural stability.

Alembagheri (2016) a developed new method to evaluate structural damage seismic, which can cause to gravity dams. In this approach, the static pushover analysis was used to develop a rational and systematic approach. Three gravity dams were chosen to evaluate this approach. To estimate the damage condition of these dams, 12 real seismic ground motions were scaled to increase the intensity levels, and the nonlinear time-history analysis was used to confirm the obtained results. Therefore, a damage index was developed to objectively anticipate the seismic damage of gravity dams.

Zacchei *et al.* (2017) examined the earthquake risk behaviour of Rules Dam, in Spain, and its effect on this body's dam, the basin, and the interface fluid structure. In this numerical investigation, the largest soil acceleration was recorded twice the results based on the Spanish code. Three controlling earthquakes have been chosen to determine the seism's primary properties. The dam study utilized various software to estimate multiple parameters. Time-history studies have been done to examine the repercussions of a collapse and to predict small damage acceptance. The results of the study demonstrate that the stresses surpass the tensile limit permitted for manufacturing plastic hinges.

Fu *et al.* (2018) proposed a numerical measure to estimate the stresses and damages of an arch dam due to earthquake waves. Although, they provided an appropriate method to enhance its behaviour against earthquakes. The obtained numerical results were compared with the previous studies concerning the displacement of the arch dam in the three directions. The frequency of the arch dam was also shown in this study with and without the water pressure of the reservoir; it showed a 26.99% difference between the two cases. The enhanced measure provided in this study is quite efficient.

Xu *et al.* (2020) studied the damages that occurred to the Baihetan arch dam, in China, after being hit by several stochastic earthquakes. Seismic behaviour assessment was accomplished using a nonlinear endurance time study. The predictable correlations between compression joint opening, displacement, and damage volume ratio were found by applying a multimodal modelling approach. The findings of correlation and fragility analysis revealed that damage volume ratio and the sum of joint opening were consistent, which gave a good scientific basis for anticipating earthquake damage.

Messaad *et al.* (2021) studied numerically the dynamic performance of the dam-reservoir-foundation for Oued Fodda dam in Algeria, due to seismic load. The stiffness of the foundation should be considered in the study of the dam, to be able to inspect the critical response of the dam foundation response. The achieved research suggests that the foundation soil leads to smaller displacements in the dam body and minimizes the primary stresses, as well as shear stresses, when Young's modulus for both the dam and foundation were equivalent.

Pasbani Khiavi *et al.* (2021) examined the responses to achieve the optimal body stiffness using probabilistic and uncertainty methods after evaluating the effect of Young Modulus of both the body concrete and the foundation as strength parameters for concrete arch dams. The dam-reservoir-foundation system's finite element analysis was completed using ANSYS software, and the Monte Carlo method, a new method for parametric study and sensitivity analysis, was used for uncertainty analysis. The dam's safety status can be investigated using the design criteria, and the best state for the model in terms of structural strength can be chosen. However, in order to properly select the modulus of elasticity of the dam body concrete, the simultaneous effect of the stiffness of the foundation must be considered and the optimal value chosen.

Daneshyar *et al.* (2021) presented a finite element model for a comprehensive nonlinear seismic simulation of a concrete gravity dam, including realistic ground-structure interactions. According to this study, a rigorous nonlinear finite element model requires an accurate description of the material response. The Koyna gravity dam was analyzed based on various assumptions about foundation, concrete reaction, and reservoir conditions. A comparison of the responses obtained under conventional assumptions with the results of the comprehensive model presented demonstrates the importance of considering radiation attenuation and the need for a rigorous constitutive materials model according to the model presented.

Xue *et al.* (2022) compared the seismic responses of the arch dam during stimulation from the plan response zone under new and old standards. The dynamic computation was conducted on a three-dimensional finite element procedure. The effect of this study showed the reflection of the characteristic period and attenuation index. The results revealed that the dynamic stressful situations of the arch dam, during stimulation from the model response spectrum in the new set of standards, were higher as compared to the old standard. The seismic stability of an arch dam may diminish under stimulation from the planned response spectrum in the revised standard. Thus, the seismic validation on constructed arch dams should be performed by adopting the new standard where it is practicable.

This paper presents a numerical study of a proposed medium arch dam subjected to an earthquake. The primary goal of this research is to show the effect of earthquake forces on a medium arch dam, using the 'pseudo-static method' (PSM). The obtained results will be compared with the 'response spectrum method' (RSM). Numerical results were obtained using the Advance Design program. The dam was designed and constructed based on concrete material mainly. The nature of this used material has a higher resistance in compression and meager resistance in tensile stress. In this case, the tensile stresses should be verified; otherwise, the concrete will be cracked. The water load will overcome the dam, due to these cracks, and could subjected it to a catastrophic failure. For this reason, and referring to Anton *et al.* (2019), the maximum tensile stress ($\sigma$) in the designed dam should be less than 8 MPa:

$$\sigma = \frac{p_{av} \times r_{av.}}{e_{av.}} \tag{1}$$

$$p_{av} = p \times \left(1 + \frac{e_{av}}{2 \text{ x } r_{av}}\right) \tag{2}$$

with

$P$ = Water pressure.
$P_{av}$ = Average water pressure.
$r_{av}$ = Average radius.
$e_{av}$ = Average thickness.

## 2. METHODS

The probabilistic seismic hazard approach (PSHA) is considered one of the oldest earthquake mathematical methods as discussed by Cornell (1968), and later by Reiter (1990). It was widely used to evaluate seismic behaviour. Two main variables key for this method are used, regression coefficients and standard deviation. Regardless of the good outcomes of the advances achieved in the usage of this approach, there are still inconsistencies related to the derivate curves. The mathematical models of seismic activity have a great effect on the conclusions derived from the used seismic hazard studies in reality. This interpretation justifies the initiatives taken by several researchers worldwide in the design of different mathematical simulations. Such methods were based on recorded data for catastrophic earthquakes. As a result, there is a variety of alternative mathematical models for evaluating earthquake shaking. Two mathematical methods were chosen to study the effect of an earthquake on a medium arch dam.

### 2.1. Pseudo-static method (PSM)

In the past, seismic design studies the behaviour of soil embankment dams and slopes by applying a body modification force. The seismic load applied to a concrete dam was considered a pseudo-static load. This old method was an easy one since the technology was not well developed in the past as now. This method considers the inertia force of the dam, and the hydrodynamic forces, which developed from water waves (Nath 1971; Melo & Sharma 2004; Pasbani Khiavi & Sari 2021). The weight of the theoretical sliding mass '**M**' and the seismic coefficient '**k**' are used to measure the magnitude of the static inertial load, which represents the seismic load '**F**'. According to Alembert's principle, the inertia load of the dam is represented by this formula:

$$\mathbf{F} = \mathbf{k} \times \mathbf{M} \tag{3}$$

$$\mathbf{F} = \mathbf{k} \times \mathbf{V} \times \boldsymbol{\gamma}_\mathbf{b} \tag{4}$$

where:

$$\mathbf{k} = \boldsymbol{\alpha} \times \mathbf{a}_{\mathbf{max}}/\mathbf{g} \tag{5}$$

with

$\mathbf{k}$ = Pseudo-static coefficient.
$\boldsymbol{V}$ = Volume of the concrete.
$\gamma_\mathbf{b}$ = Specific weight of concrete.
$\mathbf{a_g}$ = Maximum acceleration.
$\mathbf{a}$ = Seismic coefficient = 2/3 for the horizontal component.
= 0.2 for the vertical one.

when an earthquake occurs, the dam will bound against the upstream pressure of the water of the reservoir. The water force inertia will generate additional water pressure on the upstream face of the dam. This additional pressure is recognized as hydrodynamic pressure. Westergaard (1933) suggested a parabolic formula to describe this phenomenon (depend on the **h** depth of the hold, **k** pseudo-static coefficient, and $\gamma_w$ specific weight of water).

$$(\mathbf{y}) = \frac{\mathbf{7}}{\mathbf{8}} \times \mathbf{k} \times \gamma_{\mathbf{w}} \times (\mathbf{h} \times \mathbf{y})^{0.5} \tag{6}$$

The hydrodynamic force will be added to the upstream water pressure. A final formula will obtain by substituting **k** in the Equation (3):

$$\mathbf{F} = \frac{\mathbf{7}}{\mathbf{12}} \times \mathbf{k} \times \gamma_{\mathbf{w}} \times \mathbf{h}^2 \tag{7}$$

This load will be applied at 2/5 of the total height of water as shown in Figure 1.

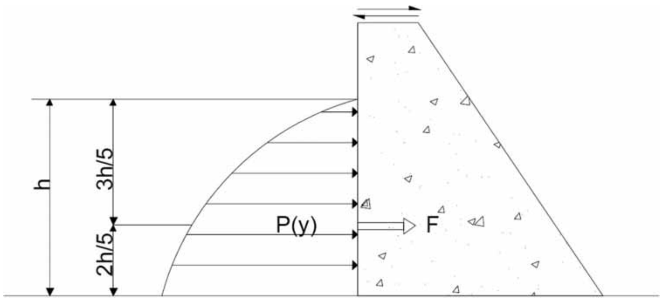


**Figure 1** | Seismic load defined by Westergaard.

### 2.2. Response spectrum method (RSM)

The second method used for this study is the Response Spectrum method. This method was introduced by Biot (1932). Recently, it was used by Løkke & Chopra (2014), and Hariri-Ardebili & Saouma (2018). It is a way of detecting earthquake reactions of buildings utilizing waves or vibrational configuration forms. The force distribution is based on natural vibration modes into this case. This method is a precise method that takes in consideration the real dynamic force produced due to an earthquake. It is based on the determination of the response of the dam over dynamic force. Each eigenmode has its mass, frequency, acceleration, and period.

In the mid-twentieth century, design specifications, such as California's building codes, incorporated the 'response spectrum method'. As strong-motion accelerograph datasets became commonly available in the 1970s, they became widely used as the principal theoretical tool in earthquake engineering (Trifunac & Todorovska 2008).

To evaluate the modal response, the acceleration will be multiplied by the modal mass of each mode. The spectral modal analysis consists of determining the modal mass of the studied system. Successive steps should be followed to obtain the results. The most common type of analysis is quasi-static analysis, where the load is applied at a very slow rate so that the acceleration is negligible. After that, the eigenmodes of the structure is defined, by searching for a normal mode of vibration of an oscillating system. Then, by selecting useful modes, the corresponded modal responses will be estimated.

To study the response of the modes, the modes should be selected with a modal mass greater than 5% of the total vibrated mass. While the sum of the masses of each mode chosen should be at least 90% of the total mass of the dam ($\Sigma Mi > 90\%$) (EN 1998-1: 2004). Moreover, the needed modal responses should be integrated independently in each mode, to study any kind of variable due to the seismic force.

The periodic modal responses are combined with the seismic effects of the different studied directions of the earthquake: There are two combination methods to achieve that: Complete Quadratic Combination (CQC) or Square Root of Sum of Squares (SRSS).

The two periods $\mathbf{T_i} \leq \mathbf{Tj}$ have two modes i, and j. These two modes are considered either independent or dependent. They will be considered dependent if they satisfy the following condition:

$$\boldsymbol{T_J} \leq \mathbf{0.9}\boldsymbol{T_i} \tag{8}$$

Otherwise, they are considered dependent, and the SRSS combination is used as follows:

$$\boldsymbol{S} = \pm\sqrt{\Sigma \boldsymbol{S_i}} \quad (9)$$

The seismic force has three possible directions X, Y, and Z. Each direction has its combination. Newmark's rule (100%–40%–40%) means that each direction is combined with 40% of the other directions. Those combinations were defined as follows:

$$\boldsymbol{S} = \boldsymbol{SX} \pm 0.4\boldsymbol{SY} \pm 0.4\boldsymbol{SZ} \quad (10)$$

$$\boldsymbol{S} = \boldsymbol{SY} \pm 0.4\boldsymbol{SX} \pm 0.4\boldsymbol{SZ} \quad (11)$$

$$\boldsymbol{S} = \boldsymbol{SZ} \pm 0.4\boldsymbol{SY} \pm 0.4\boldsymbol{SX} \quad (12)$$

**SX**, **SY**, and **SZ** are the stresses at each of the horizontal and the vertical earthquake components, while S is their resultant (Nie *et al.* 2010).

A dam has mainly two thicknesses, one at the crown noted $\mathbf{e_c}$, and another at the base noted $\boldsymbol{e_b}$. Following the recommendation of the US Bureau of Reclamations (USBR) for an arch dam, the height will be divided into three sections (Boggs 1977; Manual No. 1110-2-2201 1994). In addition to the previously cited thicknesses, and due to this division, another thickness at 0.45 of the height will be determined ($\boldsymbol{e}_{0.45}$). These thicknesses were found in the function of the dam's height and vary consensus to the valley:

$$\boldsymbol{e_c} = 0.01 \times \left(\boldsymbol{H} + \frac{1}{2} \times \boldsymbol{L}_1\right) \quad (13)$$

$$\boldsymbol{e}_{0.45} = 0.95 \times \boldsymbol{e_b} \quad (14)$$

$$\boldsymbol{e_b} = \left[0.012 \times \boldsymbol{H} \times \boldsymbol{L}_1 \times \boldsymbol{L}_2 \times \left(\frac{\boldsymbol{H}}{122}\right)^{\left(\frac{\boldsymbol{H}}{122}\right)}\right]^{\frac{1}{3}} \quad (15)$$

where $\boldsymbol{L_1}$, $\boldsymbol{L_2}$: Lengths found in the strings of the dam.

$\boldsymbol{H}$: Static height of the dam.

To facilitate the calculations, and regarding the geometry of the valley, empirical formulas were used (Anton *et al.* 2019)

$$\boldsymbol{e_c} = \frac{\boldsymbol{H}}{20} = \frac{30}{20} = 1.5\mathbf{m} \quad (16)$$

$$\boldsymbol{e_c} = \frac{\boldsymbol{L_c}}{15} = \frac{120}{15} = 8\mathbf{m} \quad (17)$$

$$\mathbf{e_{av}} = (1.5 + 8)/2 = 4.75\mathbf{m}$$

### 2.3. Case study analysis

The arch dams were categorized referring to their elevation (Breeze 2018). A dam was considered a small one if its height was below 30 m. While the height was above 90 m, it will be a tall dam. Otherwise, the dam was classified as a medium one, (height is between 30 m and 90 m). In the stress calculation, the membrane approach is appropriate for computer modelling of the arched dam. The loads were arranged in a circular pattern. In this case study, Mseilha arched dam with its 30 m executed height to satisfy satisfied the medium type condition. This medium dam has a massive central concrete structure, catchment area of 189 $km^2$, reservoir volume of 7,500,000 $m^3$, volume of backfill: 1,150,000 $m^3$. The project comprises the construction of a 30,000 $m^3$/day water treatment facility. This arched dam rested on a V-shaped valley in North Lebanon with a length at the crown $\mathbf{L_{ca}} = 120$ m, and a length at the base $\mathbf{L_{cb}} = 16$ m (MoE 2020). The slenderness ratio (λ) which is the ratio between the crown length to the dam height:

$$\boldsymbol{\lambda} = \frac{\mathbf{L_{ca}}}{\mathbf{H}} = \frac{120}{30} = 4 \tag{18}$$

Following the recommendation of Eurocode, this ration should be less than 5, so it was verified.

Another two dimensions should be distinguished, $\mathbf{r_{c1}}$ and $\mathbf{r_{c2}}$. Referring to the geometry of the arched dam, two angles were obtained. The crown-opening angle ($2\beta_c$) was 120°, while the opening angle at the base ($2\beta_b$) was 80°. The values of the radius could be calculated using the following formula:

$$r_c = Lc/2\sin\beta \tag{19}$$

$$r_{ca} = Lc\ /2\ \sin\ \beta_c = 120/2 \times \sin(60^\circ) = 69.28\text{m}$$

$$r_{cb} = Lc\ /2\ \sin\ \beta_b = 120/2 \times \sin(40^\circ) = 12.45\text{m}$$

$$r_{av} = (69.28 + 12.45)/2 = 40.865\text{m}$$

All the used dimensions are shown in Figure 2.

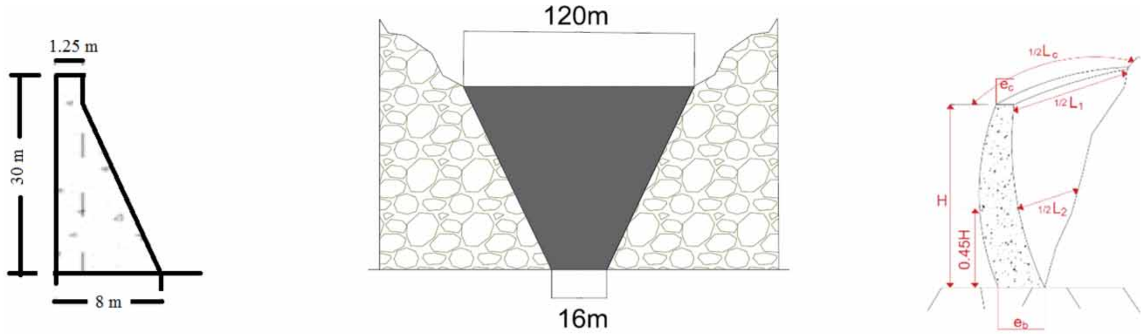


**Figure 2** | Arch dam dimensions.

In order to check that all the dimensions will be secure, the stresses should be verified before modelling the proposed medium dam.

Referring to Equations (1) and (2), in addition to Figure 2, the stresses of the proposed medium dam can be calculated as following:

$$P = 10 \times \left(\frac{25 \times 25}{2} - 300\right) = 125\ kN/m$$

$$P_{av} = 125 \times \left(1 + \frac{4.75}{2\ x\ 40.865}\right) = 132.2\text{kN/m} = 0.132\ \text{MPa}$$

$$\sigma = 0.132 \times \frac{0.132\ \times 40.865}{4.75} = 1.137\text{MPa} < 8\ \text{Mpa.}$$

The stresses exerted by the water on the proposed medium arch dam is acceptable, and the dam can resist it. The forces exerted on the dam are were the upstream pressure, the sediment pressure, the weight of the dam, and the seismic load that was represented by a pseudo-static force in the first study.

Advance Design (2022) finite element analysis software developed for the civil engineering domain, provides a complete platform from structure simulation to post-processing results, and structure modification. It covers a full variety of features specialized in sophisticated CAD models, meshes generation, analysis, validation, and improvement of concrete, metal, and wood constructions, resulting from post-processing and production of high-quality outputs.

Advance Design uses the main worldwide standards (Eurocode, North America…). In this case, this software was used to calculate the stresses of the dam consider first the pseudo-static force applied to the dam. Although, the frequencies and modes of the dam. The analysis in the Advance Simulation model is established in four operational modes: Models, Analyse, Design, and Report.

The properties of each component were specified in Advance Design. Those properties are represented in Table 1.

**Table 1** | Materials properties

| Name | Value |
|---|---|
| Young's modulus E | 31,475.81 MPa |
| Rigidity modulus G | 13,114.92 MPa |
| Poisson's ratio | 0.2 |
| Compressive strength | 24.5 kN/m$^3$ |

Usually, different parts were produced in the graphical area. The option of drawing an arch on Advance Design does not exist. The model was drawn in 3D model parts as areal elements using AutoCAD software, and then the model was imported as shown in Figures 3 and 4.

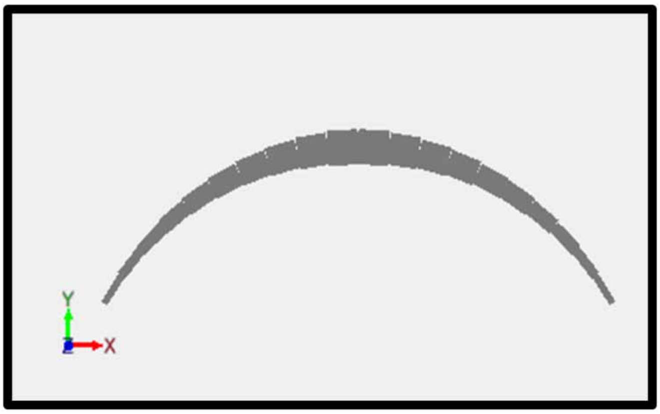


**Figure 3** | Plan view of the dam.

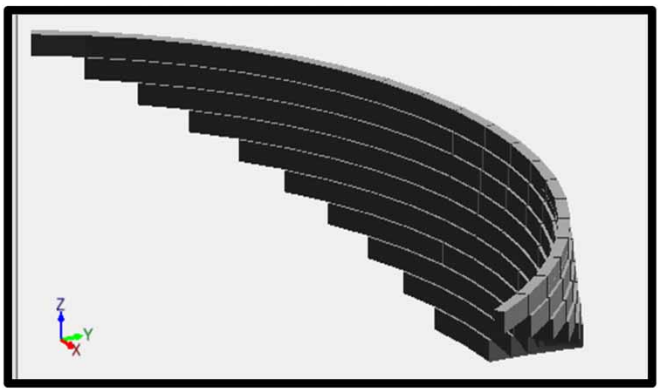


**Figure 4** | Front view of the dam.

In the pseudo-static case, the forces was added with values in two directions, horizontal and vertical. The exerted forces on the model were as follows; upstream pressure '$Q_1$' with maximum value, sediment force '$G_1$' value was 33.3 kN, the hydrodynamic force 'F' equal to 328.49 kN/m. Once all the loads were defined, the combinations were performed, and then the finite element model was analysed. During the analysis of the second case, the response spectrum, the added forces were removed (Weight of dam, sediment, and water pressure). Only the hydrodynamic force was added.

The model's consistency and integrity should be checked with the verification tool. Following the evaluation of the model, the program generates the analysis model. This model performed a numerical process that is automatically executed.

The mesh is an essential operation for the calculation of the finite element structure. The finite element meshing was accomplished using global mesh settings. The mesh parameters were specified for each element. These parameters were defined using a detailed method. This operation subdivided the structural elements into several sub-elements to refine the results of the calculation. In Advance Design, two types of mesh are available: Grid and Delaunay. In this case, the second type was used, due to its ability to build meshes for space-discretized solvers, angle guarantee, and quick development of triangulation techniques. The elements used were triangles and quadrangles (T3-Q4). The size of each element was defined by default as 0.5 m. In the end, the total node number was 3314 nodes. (Figure 5).

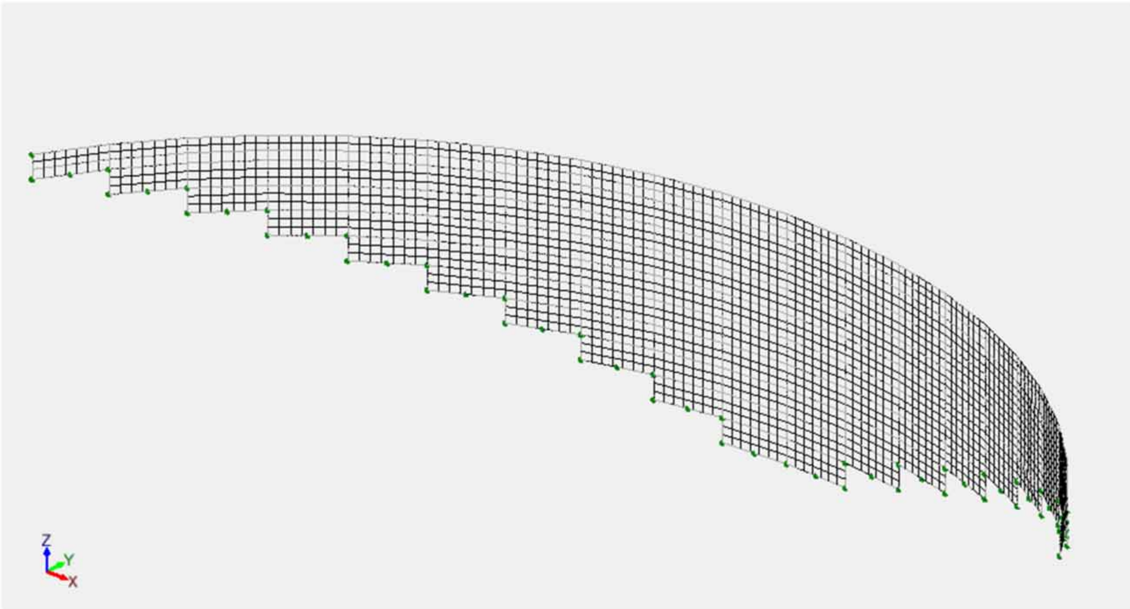


**Figure 5** | The mesh of the dam.

To calculate the stresses for this arch dam, it was divided into two parts, the consoles and the arches. The calculated stresses, in the x direction, were considered for the arch part. While, the calculated stresses, in the y direction, were considered for the console part of the dam.

Some parameters should be defined, to find the frequencies of the dam in a full reservoir state. Using the manual data of the used software (Advance Design 2022) and the recommendation of Eurocode (EN 1998-1: 2004), the parameters values were chosen as follows: the acceleration $\mathbf{a_{gr}} = 2.5\ \mathrm{m/s^2}$, the importance coefficient $\gamma_\mathbf{i} = 1$, the topographic coefficient $\mathbf{S_T} = 1.2$, and finally the depreciation correction $\boldsymbol{\eta} = 5\%$:

$$\boldsymbol{a_g = a_{gr} \times \gamma_i = 2.5 \times 1 = 2.5 m/S^2} \quad (20)$$

Advance Design permits arranging analysis in several computation stages, and computing them gradually (enable properties adjustments for each step). Six modes were chosen since the frequencies of those modes have passed the limit frequency (Figure 6). These six modes were based on the following equation:

$$\mathbf{M\ddot{U} + KU} = 0 \quad (21)$$

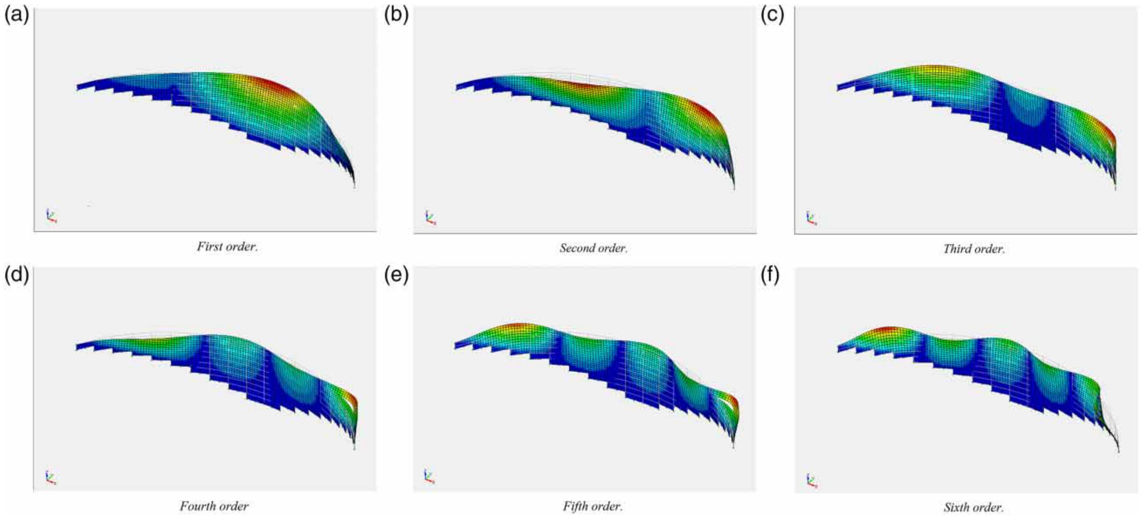


**Figure 6** | Vibration modes of arch dam under full reservoir work conditions. (a) First order. (b) Second order. (c) Third order. (d) Fourth order. (e) Fifth order. (f) Sixth order.

where: M represented the mass matrix, while K signified the stiffness matrix. $\ddot{U}$ symbolised the acceleration and $U$ the displacement.

Both of the obtained frequencies and the period's values for those modes are shown in Figure 7.

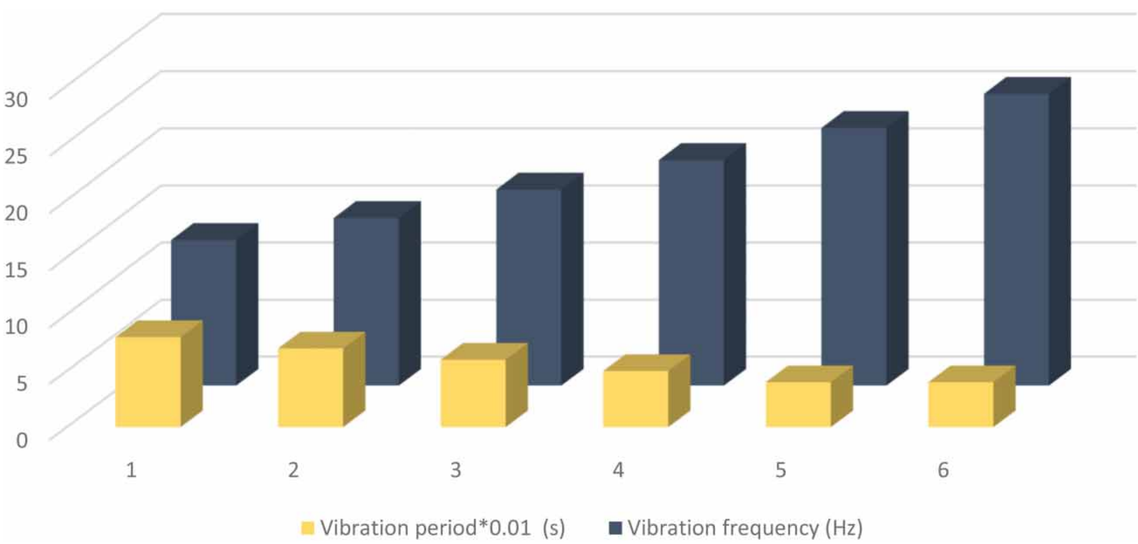


**Figure 7** | Natural vibration frequencies and periods under full reservoir conditions.

## 3. RESULTS AND DISCUSSION

After calculating the numerical effect of seismic force on proposed medium arch dam, and the variation of the stresses, then, the results should be checked and verified. The stress results according to x direction were obtained for the two parts: upstream (Figure 8) and downstream (Figure 9).

On the upstream part, it can be seen that the dam is completely compressed and that the load is transported towards the banks, which is the real case for the operation of the arch dam. The maximum stress value is in the middle of the upper part of the dark blue colour dam. The maximum compressive stress has a value of 4.13 MPa and the maximum tensile stress is 2.0 MPa. For the downstream part, the maximum compression stress has a value of 3.16 MPa and the tensile stress 1.92 MPa. This result is smaller than the compressive strength value (24.5 MPa), so it is verified.

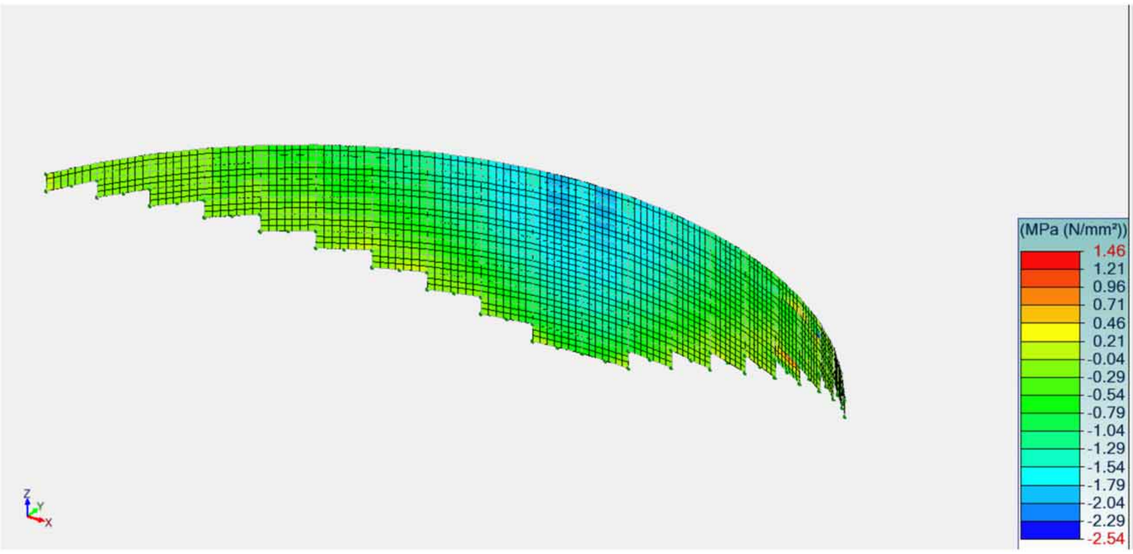


**Figure 8** | Variation of stresses along the x-axis on the upstream part.

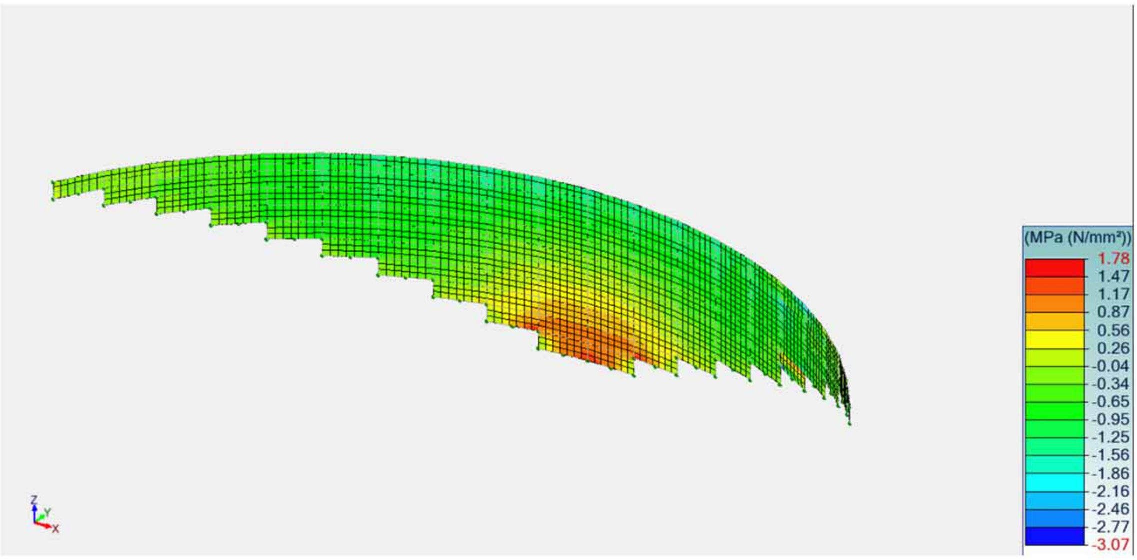


**Figure 9** | Variation of stresses along the x-axis on the downstream part.

Concerning the stress results in the y direction are determined for the two parts: upstream (Figure 10), and downstream (Figure 11). On the upstream part, we see that the dam is tense since it works like a console with maximum stress in the centre of the yellow colour of value 1.12 MPa. On the downstream part, the dam is compressed with maximum stress in the center of the dark blue colour of value 2.95 MPa.

The limit tensile stress is calculated by the following formula:

$$f_{ctm} = 0.3 * f_{ck}^{\frac{2}{3}} = 0.3 * 24.5^{2/3} = 2.53\ MPa \tag{22}$$

The results of the stresses obtained are compared to the eligible stresses of the compression and tensile stresses of the concrete used. The results also show the maximum stresses on the supports represented in Figure 12. The maximum compression stress has a value of 2.37 MPa; this value is lower than the legible stress in the foundation so it is verified. As for the tensile stress, it is too low and has a value of 0.03 MPa, it is almost zero so it does not affect the foundation.

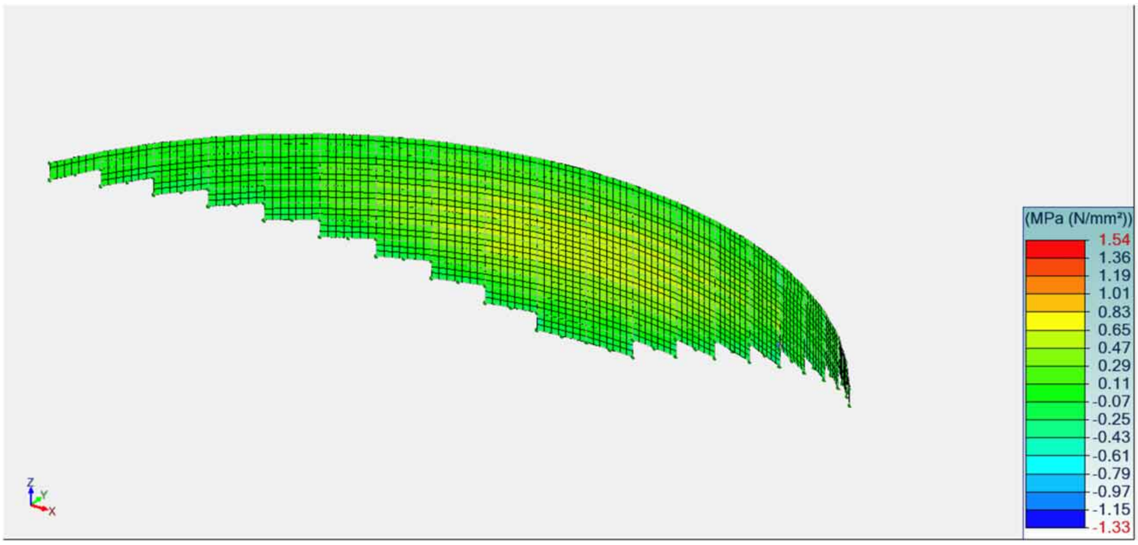


**Figure 10** | Variation of stresses along y-axis on the upstream part.

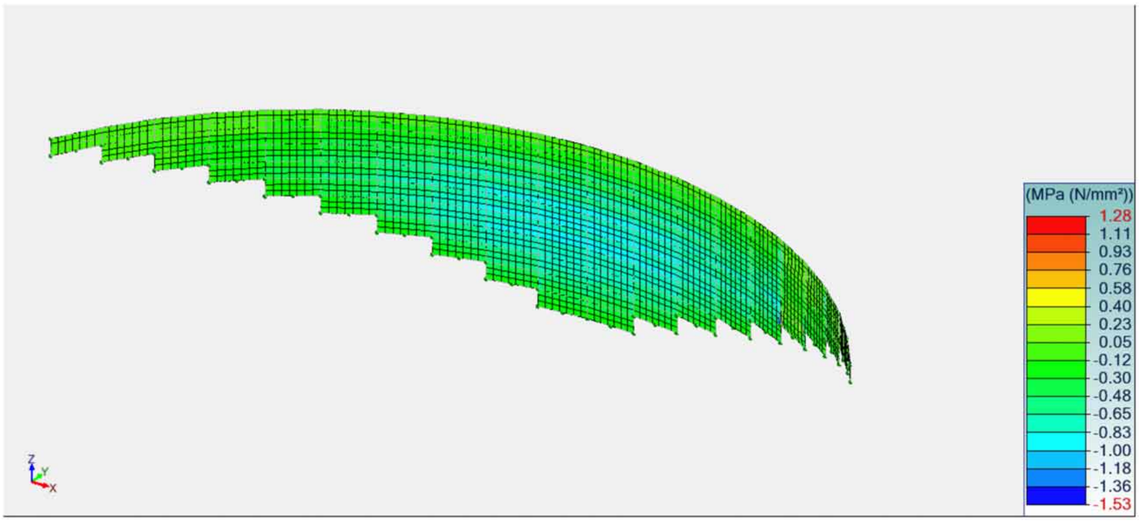


**Figure 11** | Variation of stresses along y-axis on the downstream part.

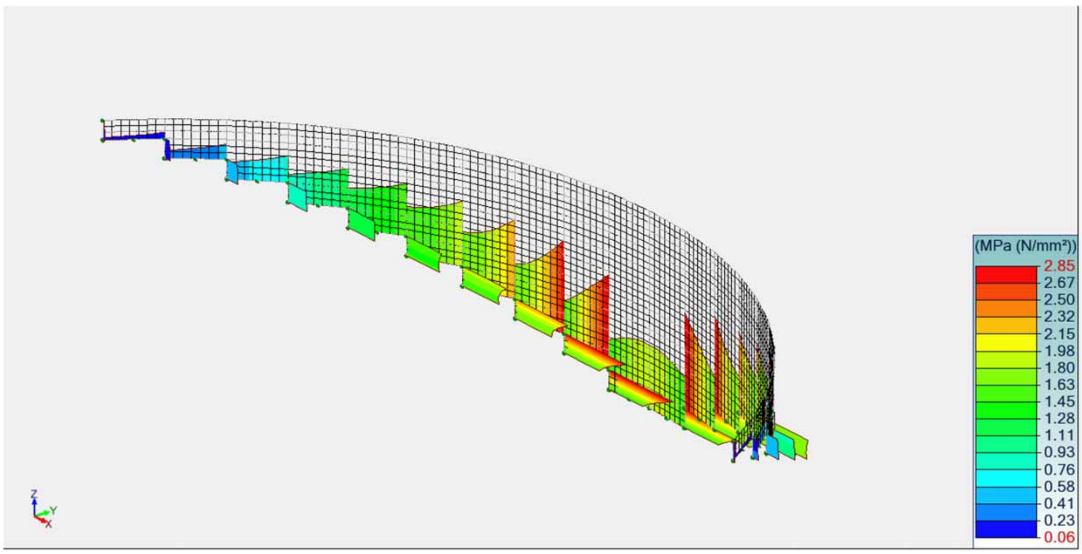


**Figure 12** | Variation of stresses under the dam.

By applying the second method of the seismic load (the response spectrum method); the values of the stresses will changed. The stress calculation results according to x direction is obtained for the two parts upstream (Figure 9), and downstream (Figure 10). The maximum stress value is in the middle of the upper part of the dark blue colour dam with a value of 6.32 MPa. The maximum tensile stress has a value of 2.97 MPa.

All the obtained results for both case studies were compared with the eligible stresses are represented in Figure 13.

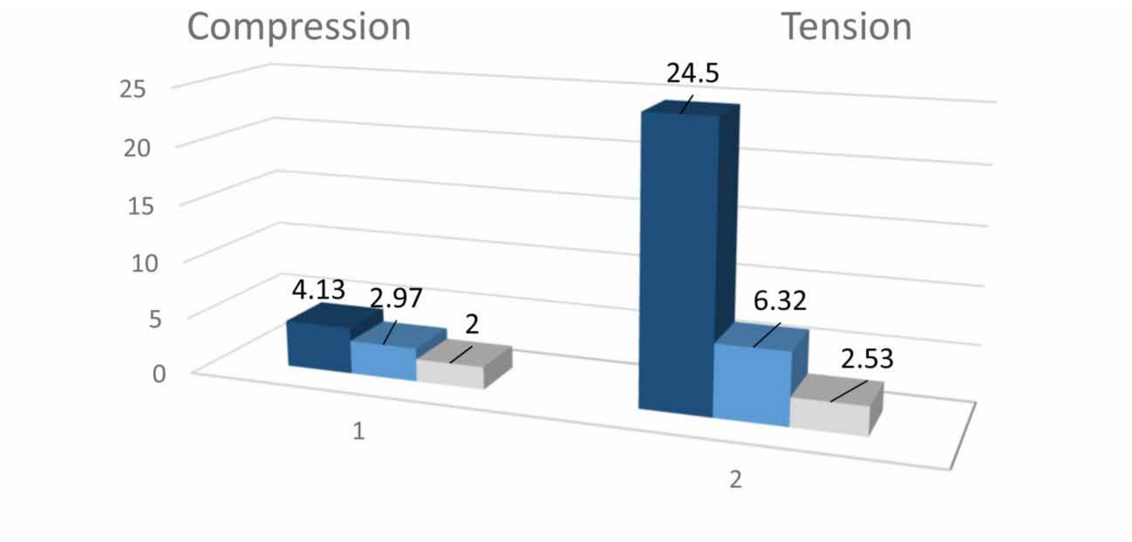


| | 1 | 2 |
|---|---|---|
| Eligible Stresses (MPa) | 4.13 | 24.5 |
| Response Spectrum (MPa) | 2.97 | 6.32 |
| Pseudo-Static (MPa) | 2 | 2.53 |

**Figure 13** | Calculated stress values compared to eligible stresses.

The obtained results for both methods (RSM and PSM) were compared with the eligible stresses. This comparison show that the stresses were within the limits. However, the stresses for the PSM were too much conservative regarding the stresses for the RSM.

## 4. CONCLUSIONS

The major necessity in seismic design for dams is to preserve safety, life, and property. This article presents a numerical overview of the impacts of the earthquake on a proposed medium dam. It clarifies the requirement of a particular design to withstand earthquakes using a pseudo-static approach. This simple method takes into account the inertial forces of the dams and the hydrodynamic pressures exerted by the reservoir.

Due to the development of computers and numerical analysis models, in the design phase and before the construction, it becomes possible to make great progress in the evaluation of the seismic safety of concrete dams. In this study, special cases was studied concerning medium dam type. For this purpose, two methods were used, the pseudo-static approach and the response spectrum method. The stresses, maximum and minimum, were found for both cases.

The maximum tensile stress, for the response spectrum method (2.0 MPa), is lower than that for the pseudo-static method (2.97 MPa) by 32.66%. The maximum compressive stress, for the response spectrum method (4.13 MPa), is lower than that for the PSM (6.32 MPa) by 34.65%.

There is an important difference between the obtained results. Various factors can be identified as explanations for the distinctions between the two seismic analysis methods. Those factors are mainly related to the added forces during numerical analysis.

Consequently, special attention should be taken into consideration in the dam design. The damages found in the dam after an earthquake can be repaired. In such cases, the solutions can be the correction of the arches' geometry to satisfy the stability conditions. Further researches should be followed to implement the obtained results with the other types of dams during the design phase.

## DATA AVAILABILITY STATEMENT

All relevant data are included in the paper or its Supplementary Information.

## CONFLICT OF INTEREST

The authors declare there is no conflict.

## REFERENCES


Advance Design 2022 *Guide de l'utilisateur*. Available from: https://docplayer.fr/9326720-Advance-design-guide-de-l-utilisateur.html (accessed 22 April 2022).

Alembagheri, M. 2016 Earthquake damage estimation of concrete gravity dams using linear analysis and empirical failure criteria. *Soil Dyn. Earthquake Eng.* **90**, 327–339. doi: 10.1016/j.soildyn.2016.09.005.

Anton, J., Schleiss, P. & Henri, P. 2019 *Les barrages du projet à la mise en service*, 17(2), 57-62, 141-175, 323, 339, 402-406. ISBN-13: 978-2880748319.

Biot, M. A. 1932 *Vibrations of Buildings During Earthquake: Transient Oscillations in Elastic System*. *PhD Thesis No. 259*, California Institute of Technology, USA.

Boggs, H. L. 1977 *Guide for Preliminary Design of Arch Dams*. Engineering and Research Centre, Bureau of Reclamation, Attention 922, Denver, USA.

Breeze, P. 2018 Hydropower. In: *Dams and Barrages*. Academic Press, pp. 23–33. doi: 10.1016/B978-0-12-812906-7.00003-X.

Chopra, A. & ASCE, M. 2012 Earthquake analysis of arch dams: factors to be considered. *J. Struct. Eng.* **138**(2), 205–214. doi: 10.1061/(ASCE)ST.1943-541X.0000431t.

Cornell, C. A. 1968 Engineering seismic risk analysis. *Bull. Seismol. Soc. Am.* **58**(58), 1503–1606.

Daneshyar, A., Mohammadnezhad, H. & Ghaemian, M. 2021 Effect of seismic wave propagation in massed medium on rate-dependent anisotropic damage growth in concrete gravity dams. *Front. Struct. Civ. Eng.* **15**, 346–363. doi: 10.1007/s11709-021-0694-z.

European Standard EN 1998-1 2004 Eurocode 8: Design of structures for earthquake resistance – Part 1: General rules, seismic actions and rules for buildings. ICS 91.120.25.

Fu, C., Zhou, H. & Pan, Y. 2018 Calculation and improvement of complex mechanical properties of the mega arch dam under multiple loads based on finite element methods. *Complexity J.* **8**, 1–12. doi: 10.1155/2018/2582561.

Harajli, M., Sadek, M. & Asbahan, R. 2002 Evaluation of the seismic hazard of Lebanon. *J. Seismolog* **6**, 257–277.

Hariri-Ardebili, M. A. & Mirzabozorg, H. 2013 Feasibility study of dez arch dam heightening based on nonlinear numerical analysis of existing dam. *Arch. Civ. Mech. Eng. J.* **59**(1), 21–49. doi: 10.2478/ace-2013-0002.

Hariri-Ardebili, M. A. & Saouma, V. E. 2018 Random response spectrum analysis of gravity dam classes: simplified, practical, and fast approach. *Earthquake Spectra* **34**(2), 941–975. doi: 10.1193/021517EQS033M.

Lee, K. L., Seed, H. B., Idriss, I. M. & Makdisi, F. I. 1975 Properties of soil in the San Fernando hydraulic fill dams. *JGED, ASCE* **101**(GT8), 801–821.

Liu, Y. S. & Chen, D. H. 2013 Earthquake response analysis of a gravity dam considering the radiation damping of infinite foundation. In *Conference APCOM & ISCM – 5th Asia Pacific Congress on Computational Mechanics & 4th International Symposium on Computation*, 11–14 December, Singapore.

Løkke, A. & Chopra, A. 2014 Response spectrum analysis of concrete gravity dams including dam–water–foundation interaction. *J. Struct. Eng.* **141**, 04014202. doi:10.1061/(ASCE)ST.1943-541X.0001172.

Madabhushi, S. P. G. & Haigh, S. K. 2005 *The Bhuj, India Earthquake of 26th January 2001: Field Report for EEFIT*. ISBN 0901297372.

Manual No. 1110-2-2201 1994 *Engineering and Design Arch dam Design*. Department of the army U.S. Army corps of engineers, Washington, DC 20314-1000.

Melo, C. & Sharma, S. 2004 Seismic coefficients for pseudostatic slope analysis paper no. 369. In *13th World Conference on Earthquake Engineering*, 1-6 August, Vancouver, BC, Canada.

Messaad, M., Bourezane, M., Latrache, M., Berrabah, A. T. & Ouzendja, D. 2021 Three-dimensional seismic analysis of concrete gravity dams considering foundation flexibility. *MCT Mech. Eng.* **25**(1), 88–98. doi: 10.2478/mme-2021-0012.

MOE: Ministry of Environment in Lebanon 2020 *Lebanon State of the Environment and Future Outlook: Turning the Crises Into Opportunities (SoER 2020)*. With UNHCR, UNICEF and UNDP, Beirut.

Nath, B. 1971 *Structural and Hydrodynamic Coupling for A Gravity dam During Vertical Earthquake Motions: Dynamic Wave in Civil Engineering*. Wiley-Interscience, Hoboken, NJ, USA.

Nie, J., Morante, R., Miranda, M. J. & Braverman, J. 2010 On the correct application of the 100-40-40 rule for combining responses due to three directions of earthquake loading. *ASME*, Pressure Vessels and Piping Division (Publication) PVP 8. doi: 10.1115/PVP2010-25466.

Pan, J., Xu, Y. & Jin, F. 2015 Seismic performance assessment of arch dams using incremental nonlinear dynamic analysis. *Eur. J. Environ. Civ. Eng.* **19**(3), 305–326. doi: 10.1080/19648189.2014.960950.

Pasbani Khiavi, M. & Sari, A. 2021 Evaluation of hydrodynamic pressure distribution in reservoir of concrete gravity dam under vertical vibration using an analytical solution. *Math. Probl. Eng.* **2021**. Article ID 6669366. doi: 10.1155/2021/6669366.

Pasbani Khiavi, M., Ahmadi, P., Daneshfaraz, R. & Abraham, J. 2021 The effect of strength parameters on the seismic performance of an arch dam using an uncertainty model. *Revista de la Construcción* **20**(3). Santiago. doi: 10.7764/RDLC.20.3.602.

Rajendran, K., Andrade, V., Natarajan, T. & Rajendran, C. P. 2011 The 11 march 2011 Tohoku (Sendai), Japan earthquake. *Curt. Sci.* **100**(7), 966–969.

Reiter, L. 1990 Probabilistic seismic hazard analysis – lessons learned: a regulator's perspective. *Nucl. Eng. Des.* **123**(2-3), 123–128. doi: 10.1016/0029-5493(90)90232-M.

Tan, H. & Chopra, A. K. 1995 Earthquake analysis of arch dams including dam–water foundation rock. *Earthquake Eng. Struct. Dyn.* **24**(11), 1453–1474. doi: 10.1002/eqe.4290241104.

Trifunac, M. D. & Todorovska, M. I. 2008 Origin of the response spectrum method. In *14th World Conference on Earthquake Engineering*, 12-17 October, Beijing, China.

Westergaard, H. M. 1933 Water pressures on dams during earthquakes. *Trans. ASCE* **98**(1835), 418–433.

Wieland, M. & Houqun, C. 2009 Lessons learnt from the Wenchuan earthquake. *Intl. W. Pwr. Dam Const. J.* September Issue, pp. 36–40. Available online: https://www.waterpowermagazine.com/features/featurelessons-learnt-from-the-wenchuan-earthquake/

Xu, Q., Xu, S., Chen, J. & Li, J. 2020 Investigation of stochastic seismic response and index correlation of an arch dam using endurance time analysis method. *Adv. Civ. Eng* 1–23. doi: 10.1155/2020/8862869.

Xue, B., Wang, J., Li, N., Zhang, C. & Chen, J. 2022 Comparison of the seismic responses of an arch dam under excitation from the design response spectrum in the new and old Chinese national standards. *Water* **14**(832), 1–12. doi:10.3390/w14050832.

Zacchei, E., Molina, J. L. & Brasil, R. 2017 Seismic hazard and structural analysis of the concrete arch dam (Rules Dam on Guadalfeo River). *Procedia Eng. J.* **199**, 1332–1337. doi: 10.1016/j.proeng.2017.09.334.

First received 7 July 2022; accepted in revised form 5 September 2022. Available online 12 September 2022